Int. J. Multiphase Flow Vol. 6, pp. 345–356
Pergamon/Elsevier, 1980. Printed in Great Britain

AIR–WATER TWO-PHASE FLOW IN A HELICALLY COILED TUBE

P. B. WHALLEY
Heat Transfer and Fluid Flow Service, AERE Harwell, Oxon., England

(*Received* 1 *August* 1979; *in revised form* 5 *February* 1980)

Abstract—Air–water flow has been studied in a helically coiled tube. The flow pattern transition between stratified and annular flow was examined, and a series of measurements were then taken in the annular flow regime. Local values of the liquid film thickness and liquid film flowrate around the tube periphery were obtained. The variations of these values around the periphery was similar. For most of the cases studied the liquid film flow rate was greatest on the inside of the bend, but in some results a subsidiary peak at the outside position was also obtained. There was little net entrained flow because of the centrifugal forces tending to deposit drops very quickly. Attempts to use correlations developed in vertical annular flow at a local position on the tube periphery were not very successful.

1. INTRODUCTION

Although a considerable amount of work has been reported on heated two-phase flow in helical coils (see for example Carver *et al.* 1964, Owhadi *et al.* 1968, Akagawa & Sakaguchi 1972, Crain & Bell 1973, Anglesea *et al.* 1974) there have been comparatively few detailed studies of the flow (see for example Banerjee *et al.* 1967 and Kozeki 1973). There has also been some relevant work performed in bends rather than helices (for example Maddock *et al.* 1974 and Anderson & Hills 1974).

In this work air–water adiabatic flow was studied in a helical coil, particular attention being placed on the annular flow regime. The results reported in this paper are given, together with additional results, in report form by Whalley & Williams (1977). This report also gives additional details of the experimental techniques used.

2. APPARATUS

A helical coil was constructed of copper tube of internal diameter (d) 20.2 mm and a wall thickness 0.9 mm. The coil (see figure 1) had a helix angle (α) of 6°, and a coil diameter (D) of 1 m. There were three complete turns between the inlet mixer and the measuring position. All

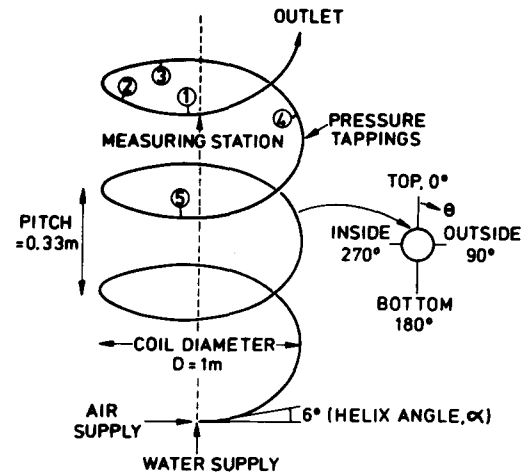

Figure 1. Helical coil.

experiments were conducted with upflow. After the measuring position there was $\frac{1}{4}$ turn before the end of the coil. At the measuring position, various straight lengths of pipe containing a viewing section, a film flow measuring device or a film thickness measuring device could be inserted. These straight sections were all of length 75 mm. The coil was later cut down to $1\frac{1}{2}$ turns to reduce the overall pressure drop. The length of the coil was found not to affect the results in any way.

After the coil had been manufactured, the average outside diameter of the tube was 21.95 mm. The largest outside diameter of the tube was usually between the inside and outside positions (see figure 1), the average value of this measurement was 22.28 mm. The smallest outside diameter was usually between the top and bottom positions, the average value was 21.63 mm.

The inlet device was a porous wall type device—a short length of the tube was made of porous sinter, and the water was forced through this sinter to join the air flow.

The details of the apparatus and methods for measuring film flow rates, film thicknesses and pressure gradients are given in the relevant sections later, and in more detail by Whalley & Williams (1977).

3. FLOW PATTERNS

A short length of perspex tube was inserted at the measuring position, and the transition between stratified flow and annular flow was observed. Here the term stratified flow is used to denote the state where the liquid flows as a film on the tube walls (this film may be quite localised and thick) but where the liquid film does not occur right round the periphery of the tube. The term annular flow is used when the liquid film does extend completely round the tube periphery. The boundary between these two flow patterns is plotted in figure 2, for an absolute pressure at the measuring position of 1.7 bar. In this figure G_G and G_L are the mass fluxes of air and water respectively; these mass fluxes are based on the total cross sectional area of the tube.

In addition the position of the film around the tube periphery was noted when the flow regime was stratified. These positions are shown in figure 3. The position of the arcs of circles indicate the positions of the film around the tube periphery. It can be seen that, for all the liquid flowrates studied, the liquid was to be found along the bottom part of the tube at low gas flowrates. As the gas flowrate was increased the effect of centrifugal force became important and the liquid film tended to be located on the inside surface of the tube. This is most clearly shown at low liquid flowrates. In some instances ($G_L = 7.9$, $G_G = 117.9\,\text{kg/m}^2\text{s}$ and $G_L = 15.7$, $G_G = 98.3\,\text{kg/m}^2\text{s}$) a separate detached film was seen on the outside of the tubes. From observations of the flow it seemed that droplets were being entrained from the main liquid film on the inside surface, and were then being deposited on the outside surface. In these two cases

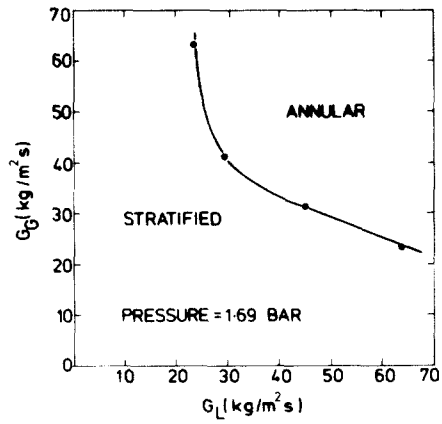

Figure 2. Boundary between annular and stratified flow.

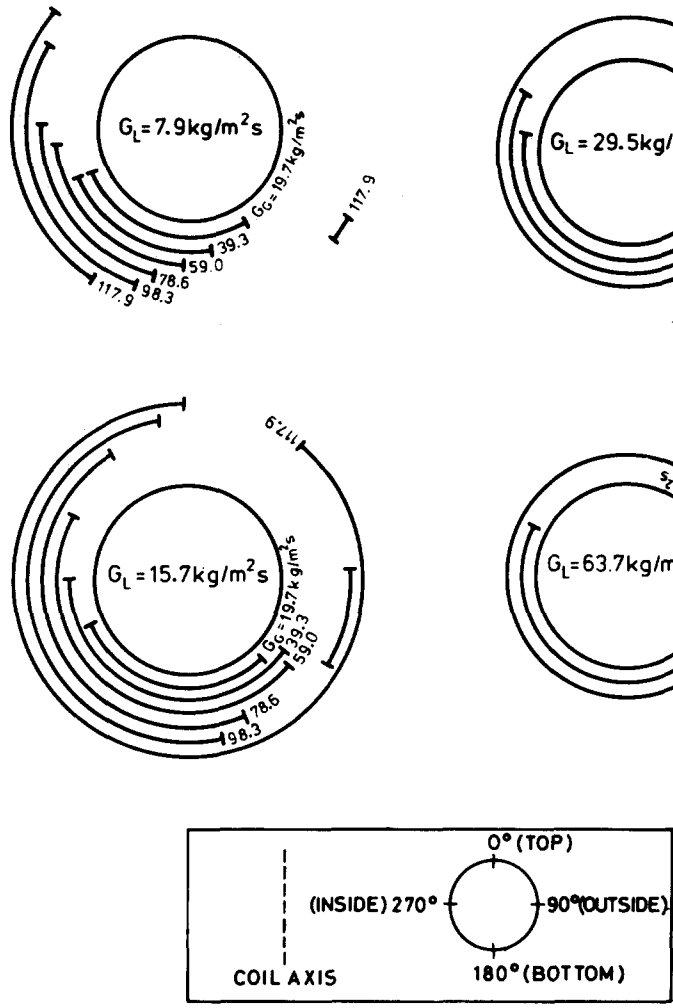

Figure 3. Position of film flow in stratified flows (P = 1.7 bar).

the deposition flux was so great that the impinging droplets formed a film on the outside surface. It should be noted that these detailed observations of the film flow position will be dependent upon the wetting characteristics of the tube surface.

4. FILM FLOWRATE

In a helical coil, like a horizontal tube, but unlike a vertical tube, the liquid film flowrate can vary substantially with circumferential position.

The film flowrate was measured by sucking off the film through a section of tube wall made of porous sinter; such a technique was used by Cousins *et al.* (1965) for vertical flow and adapted for horizontal flow by Butterworth & Pulling (1974). For vertical flow the entire periphery for an axial length of about 75 mm was sinter, but for horizontal flow only a small part of the circumference (subtending an angle of about 25° at the tube axis) was sinter. This difference is necessary so that the film flowrate in a horizontal tube can be found as a function of circumferential position.

A short section of pipe was designed incorporating a sinter similar to that of Butterworth & Pulling (1974). The sinter section differed from that used by Butterworth & Pulling in a number of ways:

(a) Because the tube diameter was smaller (20.2 mm as against 32 mm) a larger angle was subtended at the tube axis (39.6° instead of 25°).

(b) The guide vanes, which prevent liquid from peripheral locations other than those covered by the sinter from entering the sinter, project upstream from the sinter.

(c) The axial length of sinter used was shorter.

For vertical flow it has been found that the liquid flowrate sucked off through the sinter is only a weak function of the gas flowrate sucked off, but in these experiments and in the experiments of Butterworth and Pulling it was found that the liquid flowrate did increase significantly with increasing gas flowrate. If, however, the liquid flowrate at zero gas flowrate was estimated (see figure 4) this seemed to give a consistent value for the local film flowrate. The values of the liquid film flowrate obtained were reproducable to within about 5 per cent.

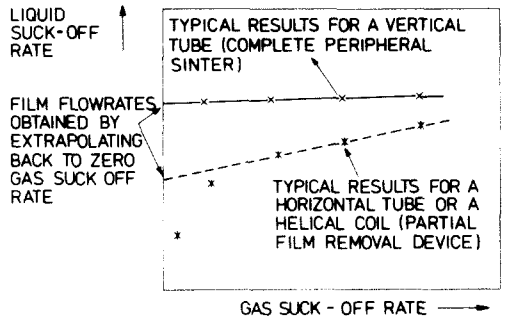

Figure 4. Liquid–gas take off characteristics of film removal devices.

Of course the local film flowrate thus obtained is an average of the actual local film flowrates at all the points falling within the 39.6° range of the sinter. Readings of the film flowrate were taken at 45°, or occasionally $22\frac{1}{2}°$, intervals. It is possible from these local average film flowrates to estimate the true local film flowrate at any point if it is assumed that these true local film flowrates on a smooth curve. This was done by estimating the true local film flowrates and then fitting a smooth curve through the points. From this smooth curve the average film flowrate over the arc covered by the sinter can be found. Discrepancies between these computed average values and measured values of the film flowrate were used to correct the estimates of the true local film flowrates.

The computed values of the local film flowrates are shown in figure 5; in this figure the experimental values of the film flowrate are shown as horizontal bars, the length of the bar representing the angular size of the sinter. From these true local film flowrate curves the mean value of the film flowrate and hence the proportion of the liquid flowing in the film can be found. The percentage of the liquid flowing in the film is given for each run in figure 5.

Figure 5 shows that:

(a) A comparatively small fraction of the liquid flow is entrained. In this work no more than 30 per cent of the liquid flows as entrained drops. The amount of entrainment generally increases, as would be expected, with both gas and liquid flowrates, though the trend with liquid flowrate is more pronounced.

(b) For most of the conditions studied, the liquid tends to travel along the inside of the coil (at $\theta = 270°$). This tendency is most marked when the gas flowrate is high and the liquid flowrate low. However when the gas flowrate is low and the liquid flowrate high, the liquid tends to travel around the outside of the coil (at $\theta = 90°$).

(c) The position of minimum flowrate is usually between $\theta = 0°$ and 45°.

(d) A subsidiary peak in the film flowrate curves can sometimes be seen at around $\theta = 90°$ (on the outer surface). This occurs when the gas flowrate is large and is particularly noticeable when the liquid flowrate is also large. This subsidiary peak is presumably due to deposition of entrained liquid drops by centrifugal force onto the outer surface.

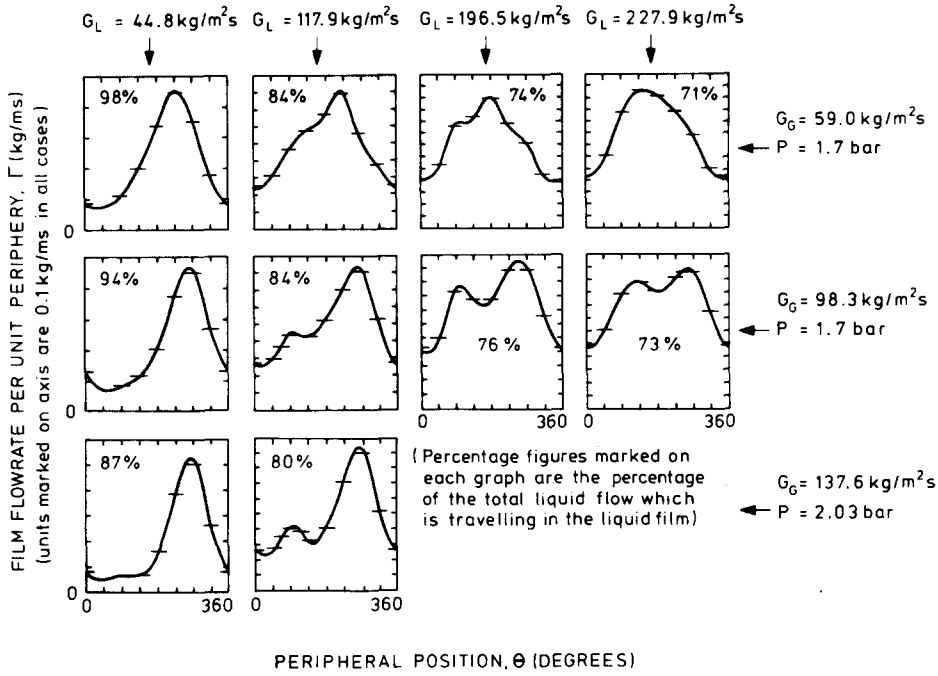

Figure 5. Film flowrates as a function of peripheral position.

5. FILM THICKNESS

In a helical coil the film thickness as well as the film flowrate varies substantially with circumferential position.

The film thickness was measured using a needle probe. This technique has been described by Hewitt *et al.* (1962) and used in a horizontal tube by Butterworth (1972) and Butterworth & Pulling (1974). A frequency counter and signal generator used to find the proportion of the time the needle is in contact with the liquid film, the probe acting as a switch between the signal generator and the frequency counter. To make the demineralised water slightly conducting a small amount of potassium nitrate was added to raise the electrical conductivity of the water to around 500 μMho/cm. From measurements of the film flowrate in these experiments and in flow in a vertical tube, this concentration of electrolyte is not believed to have significant effect on the film. The proportion of the time the needle was in contact with the film was then found for various distances of the needle from the wall. A typical plot of percentage contact time against distance is shown in figure 6.

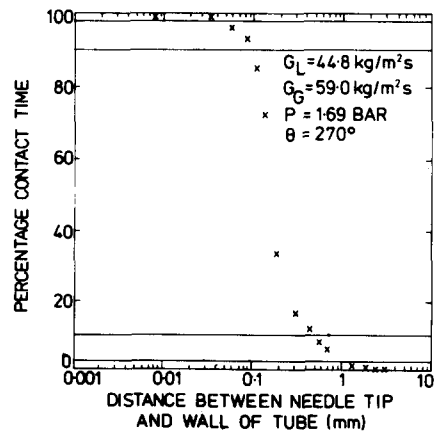

Figure 6. Typical film thickness results from needle probe.

From graphs such as this it is possible to estimate the film thickness which is exceeded for a given proportion of time. If $m_{0.02}$ is defined as the thickness which is exceeded by 2 per cent of time, then $m_{0.02}$ can be seen, from figure 6, to be equal to 1.1 mm. Similarly:

$$m_{0.1} = 0.45 \text{ mm}$$

$$m_{0.9} = 0.095 \text{ mm}$$

$$m_{0.98} = 0.035 \text{ mm}.$$

The time average film thickness, $\bar{m}$ is not equal to $m_{0.5}$, but is given by:

$$\bar{m} = \int_0^\infty p(m)\,dm, \qquad [1]$$

where $p(m)$ is the proportion of time that the film is thicker than m. For the case of figure 6, $\bar{m} = 0.247$ mm, whereas $m_{0.5} = 0.15$ mm.

Figure 7 shows the values of $m_{0.02}$, $m_{0.1}$, $\bar{m}$, $m_{0.9}$ and $m_{0.98}$ obtained as functions of peripheral angle. From the values of $\bar{m}$, the peripherally averaged mean film thickness $\bar{\bar{m}}$ could be calculated. Values of $\bar{\bar{m}}$ are also given in figure 7.

From figure 7 it can be seen that:

(a) The peripherally averaged mean film thickness, $\bar{\bar{m}}$, increases with increasing liquid flowrate, and decreases with increasing gas flowrate.

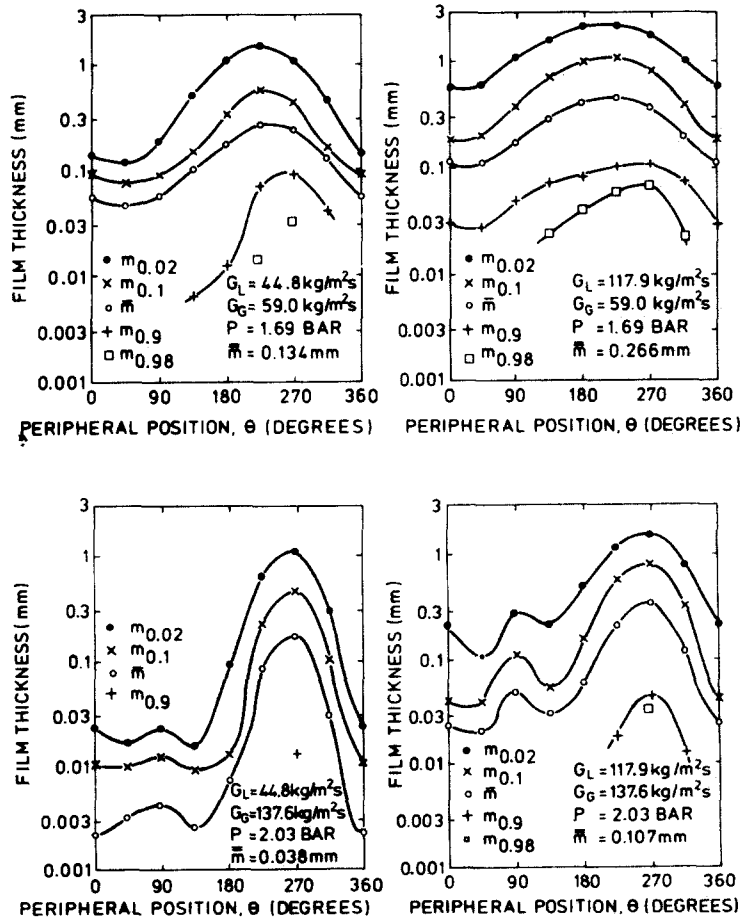

Figure 7. Film thickness as a function of peripheral position.

(b) The shapes of the curve of film thickness as a function of θ are similar to those for film flowrate. The maxima and minima occur at approximately the same positions, and those conditions which give a subsidiary peak for film flowrate, also give a subsidiary peak, for film thickness.

(c) Although the general shapes of the film thickness and film flowrate curves are indeed similar, there is sometimes a far greater difference between maximum and minimum film thickness than between maximum and minimum flowrate. For example for the conditions $G_L = 44.8\ \text{kg/m}^2\text{s}$, $G_G = 137.6\ \text{kg/m}^2\text{s}$, $P = 2.03$ bar

$$\frac{\Gamma_{max}}{\Gamma_{min}} = 10.4 \qquad \frac{\bar{m}_{max}}{\bar{m}_{min}} = 76.$$

(d) In some cases it appears from the readings from the needle probe that the film only partially wets the tube wall. For example it was found in one case that the film was thicker than 0.01 mm for only 10 per cent of the time. Observations with the visual section described earlier for the same conditions however seemed to indicate that the wall was always wetted.

6. LIQUID FILM VELOCITY

The mean liquid velocity, $\bar{U}_L$, in the film can be approximated by:

$$\bar{U}_L = \frac{\Gamma}{\bar{m}\rho_L}, \qquad [2]$$

where Γ is the computed true local film flowrate. The calculated value of $\bar{U}_L$ from [2] is shown as a function of peripheral position in figure 8. It should be noted that $\bar{U}_L$ is not the true average

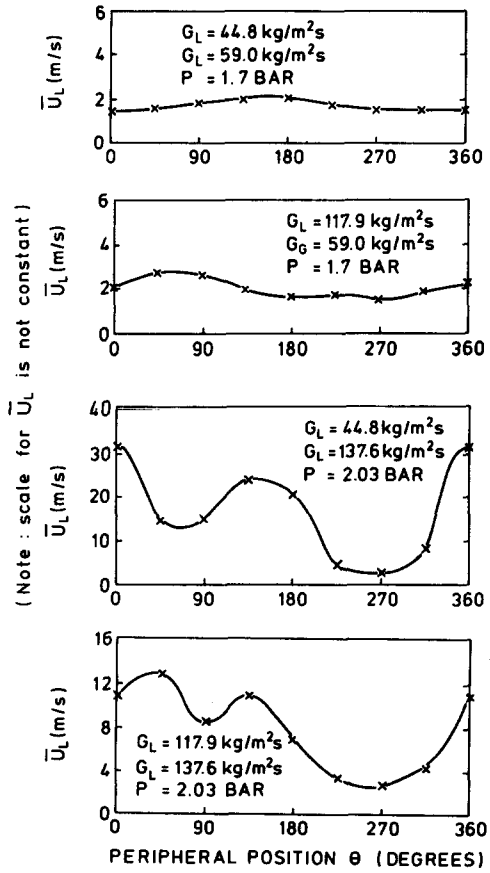

Figure 8. Calculated liquid velocity as a function of peripheral position.

liquid film velocity, to determine this it would be necessary to know something about that time variation of the film flowrate.

Figure 8 shows that the liquid velocity generally increases as the film thickness decreases for any particular flow conditions. The very high liquid velocities sometimes found (up to 30 m/s) occur when the film is very thin and the largest velocities probably correspond to the wave velocity.

7. FILM INVERSION

Banerjee *et al.* (1967) and Maddock *et al.* (1974) have considered the situation shown in figure 9. Banerjee has referred to the situation where a stratified film flows on the inside of the tube as "film inversion" and has argued that the angle δ, which is equal to θ–180°, is given by:

$$\tan \delta = \frac{2(\rho_G U_G^2 - \rho_L U_L^2)}{D(\rho_L - \rho_G)g}. \quad [3]$$

In this equation U_G and U_L are the actual velocities of the liquid and gas. Maddock *et al.* interpreted this as meaning a reasonable average velocity near the film under consideration.

For film inversion to occur:

$$\rho_G U_G^2 > \rho_L U_L^2 \quad [4]$$

or

$$U_L < U_G \left(\frac{\rho_G}{\rho_L}\right)^{1/2}. \quad [5]$$

The only estimate available of U_G is $\bar{U}_G$ the average gas velocity which would occur if the gas velocity profile were perfectly flat. $\bar{U}_G$ is given by:

$$\bar{U}_G = \frac{G_G}{\rho_G}\left(1 + \frac{4\bar{m}}{d}\right) \text{ if } \frac{4\bar{m}}{d} \ll 1. \quad [6]$$

For inversion to be consistent with the centrifugal force balance of Banerjee *et al.* the liquid velocity at the position of maximum film flow rate must respectively be less than—for experiments shown in: figure 8(a, b) 1.3 m/s, figure 8(c, d) 2.8 m/s.

Reference to these figures shows that these conditions are, or are almost, satisfied in all cases.

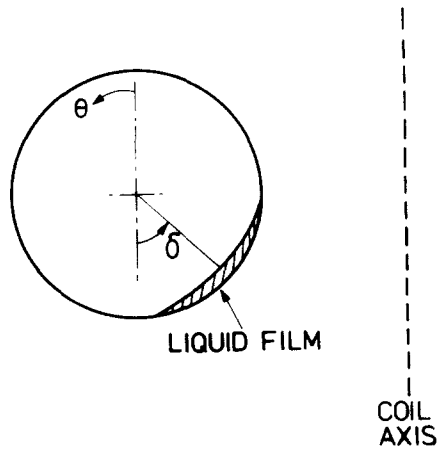

Figure 9. Film inversion.

Since inversion in the experiments described here for which film thickness measurements are available, the gas velocity near the position of maximum liquid film flowrate would be somewhat less than $\bar{U}_G$. This is because the position of maximum gas velocity is displaced from the centerline of the tube in the $\theta = 90°$ direction. As a result the condition for inversion given above is more difficult to satisfy. It is thus impossible to give a clear indication whether the inequality [5] for inversion is effective or not.

8. PRESSURE GRADIENT

Pressure tappings consisting of a 1 mm hole were located at the inside position ($\theta = 270°$) at five locations in the coil. These are shown in figure 1. The distance measured along the tube centre line between tapping number 1 and the centre of the measuring station was 160 mm. The distance again measured along the tube centre line, between tapping number 1 and the other tappings are shown below:

Tapping number	Distance from tapping 1 (mm)
2	487
3	980
4	2006
5	2981

The pressure differences between tapping 1 and the other tappings were measured by the water purged manometer technique described by Hewitt *et al.* (1962). In evaluating the pressure difference from the manometer reading, the difference in vertical height between the tappings was taken into account. The pressure differences were measured at the same flow conditions that were used for the film flow and film thickness experiments described earlier. The pressure gradient results were plotted against the distance between the two tappings, and extrapolated to give an estimate of the local pressure gradient at tapping 1. No attempt was made to estimate the local pressure gradient at the position where the film flowrate and film thickness was measured as the distance between this point and tapping 1 was quite short.

The extrapolated values of the pressure gradients can be divided into frictional, accelerational and gravitational components. The gravitational component $(dP/dz)_G$ can be estimated from the equation:

$$\left(\frac{dP}{dz}\right)_G = \frac{4\dot{m}}{d} \cdot \rho_L g \sin \alpha. \qquad [7]$$

Here the density of the gas has been neglected in comparison to the liquid density. The contribution of the entrained liquid droplets to the liquid hold-up has also been neglected in comparison to that of the liquid film. The values of $(dP/dz)_G$ calculated in this way are, at most, about 1 per cent of the total pressure gradient.

The accelerational component $(dP/dz)_A$ could, in principle, be divided into parts: that caused by changes in the liquid momentum flux, and that caused by changes in the gas momentum flux. Changes in the liquid momentum flux, at least for the liquid in the film, cannot be calculated as the liquid velocities were only determined at a single pressure for each flow condition. However as the average gas velocities are very much greater than the average liquid film velocities the dominant term is likely to be that concerned with changes in gas momentum flux. Making this assumption, and the further assumption that the voidage can be taken as unity, the accelerational pressure gradient can then be written as:

$$\left(\frac{dP}{dz}\right)_A = \frac{G_G^2}{P\rho_G}\frac{dP}{dz}, \qquad [8]$$

where dP/dz is the total pressure gradient. Values of $(dP/dz)_A$ calculated from [8] are, at most, less than 4 per cent of the total pressure gradient.

Thus the frictional pressure gradient is the dominant component in the total pressure gradient.

9. SHEAR STRESS CALCULATION

It is well known (see for example Hewitt & Hall Taylor 1970) that there is a comparatively well tested relationship, the triangular relationship, in annular flow between three of the main dependent variables: average film thickness ($\bar{m}$), film flowrate (Γ) and wall shear stress (τ_0). Butterworth (1974) quotes a particularly simple form of the relationship which is based on the universal profile.

$$\Gamma^+ = \tfrac{1}{2}(m^+)^2 \text{ for } m^+ \leqslant 5 \quad [9a]$$

$$\Gamma^+ = 12.5 - 8.05m^+ + 5m^+ \ln m^+ \text{ for } 5 < m^+ \leqslant 30 \quad [9b]$$

$$\Gamma^+ = -64 + 3m^+ + 2.5^+ \ln m^+ \text{ for } m^+ > 30 \quad [9c]$$

where m^+ and Γ^+ are dimensionless film thickness and film flowrate given by

$$\Gamma^+ = \Gamma/\mu_L \quad [10]$$

$$m^+ = \bar{m}(\tau_0\rho_L)^{1/2}/\mu_L \quad [11]$$

where μ_L is the liquid viscosity.

There seems no reason why [9] should not be valid locally at a given peripheral position. To test this assumption the experimental values of time averaged local film thickness and local film flowrate were used to calculate, from [9] to [11], a value for the local shear stress. The local shear stresses could then be averaged around the tube periphery and a value of the frictional pressure gradient produced, which could be compared with the experimental value. In fact the experimental total pressure gradient was used as this was very nearly equal to the frictional component.

The results of the above procedure are disappointing—even with experimental conditions where the film thickness is relatively large, the pressure gradient is over-predicted by a factor of 2 or 3. When the film thicknesses are very small the calculated pressure drop is up to 200 times too large; however, this latter result is not too disturbing as it is likely that the film is only intermittently present in these cases. It would be expected that the analysis would only be valid for a continuous film.

If attention is now restricted to the cases where the liquid velocities show no sign of large increases due to intermittent films, it is found that increasing the experimental film thicknesses uniformly by a factor of 1.7 ± 0.25 will give good results for the pressure gradient. Some error will of course be present in the experimental film thicknesses, particularly as the values were to some extent sensitive to the noise rejection level on the frequency counter. However it is thought unlikely that the errors were large enough to account for the discrepancy in pressure gradient.

The calculated values of the shear stress are found to vary substantially around the tube (often by a factor of 4 or more), generally the calculated values are large when the experimental values of film thickness and film flowrate are low. A similar result is found if the horizontal annular flow results of Butterworth & Pulling (1973) are similarly analysed, but Pulling (1975) and Fisher & Pearce (1979) have found experimentally that in horizontal flow the shear stress was relatively constant around the tube periphery. Moreover the shear stress was highest when the film flowrate and the film thickness were high. There is a contradiction here: either the triangular relation, as used here, is not a good description of the film behaviour, or the shear stress does vary considerably around the tube periphery.

It is possible that if the triangular relation were applied in a more complex manner, so that the circumferential flow was introduced, the results might be more satisfactory. Such a calculation would however be even more complicated than for the case of horizontal annular flow (see for example Hutchinson *et al.* 1974 and Fisher & Pearce 1979) because the secondary flow in the gas phase certainly could not be neglected. It is also possible that the high deposition and entrainment flux of droplets in certain parts of the liquid film render the triangular relationship inapplicable.

10. CONCLUSIONS

The local film flowrate, local film thickness and pressure drop for air–water flow in a helically coiled tube have been measured. For many of the flow conditions studied the liquid tended to travel as a film along the inside surface, but it was not possible to verify inequality [5] for the existence of this type of flow pattern. Attempts were made to test the triangular relationship for annular flow in helically coiled tube, but again it was not possible to come to any conclusion. The measurement of local wall shear stresses would seem necessary to resolve the current uncertainty.

Acknowledgements—This work was supported by the Chemical and Minerals Requirements Board of the U.K. Department of Industry, and was part of the research programme of the heat Transfer and Fluid Flow Service operated jointly by the National Engineering Laboratory and A.E.R.E. Harwell.

NOMENCLATURE

d	tube diameter, m
D	coil diameter, m
dP/dz	total two-phase pressure gradient, N/m^3
$(dP/dz)_A$	accelerational component of the two-phase pressure gradient, N/m^3
$(dP/dz)_G$	gravitational component of the two-phase pressure, N/m^3
g	acceleration due to gravity, m/s^2
G_G	mass flux of gas (mass flowrate of gas/total cross sectional area of the tube), kg/m^{2}s
G_L	mass flux of liquid (mass flowrate of liquid/total cross sectional area of the tube), kg/m^{2}s
m	film thickness at a certain peripheral position, m
m^+	dimensionless value of film thickness corresponding to $\bar{m}$
$\bar{m}$	average film thickness at a certain peripheral position, m
$\bar{\bar{m}}$	peripherally averaged value of $\bar{m}$, m
$m_{0.02}$, $m_{0.1}$, etc	values of the film thickness at a certain peripheral location which are exceeded for 2, 10 per cent, etc. of time, m
P	absolute pressure, N/m^2
U_G	local gas velocity, m/s
$\bar{U}_G$	mean gas velocity, m/s
U_L	local liquid velocity, m/s
$\bar{U}_L$	mean liquid velocity, m/s
α	helix angle
δ	angle in figure 9
θ	peripheral angular position
μ_L	liquid viscosity, Ns/m^2
ρ_G	gas density, kg/m^3
ρ_L	liquid density, kg/m^3
τ_0	wall shear stress, N/m^2

Γ film flowrate (mass per unit time per unit periphery), kg/ms
Γ^+ dimensionless film flowrate

Subscripts

max maximum value around periphery
min minimum value around periphery

REFERENCES

AKAGAWA, K & SAKAGUCHI, T. 1972 Frictional pressure drop in steam generating tubes. *Bull. J. SME* **15**(80), 264–276.

ANDERSON, G. H. & HILLS, P. D. 1974 Two phase annular flow in tube bends. Symp. Multi-phase Flow Systems, University of Strathclyde, Glasgow, Paper J1, Published as Instn. Chem. Engrs. Symp. Series No. 38.

ANGLESEA, W. T., CHAMBERS, D. J. B. & JEFFREY, R. C. 1974 Measurements of water/steam pressure drop in helical boils at 179 bars. *Symp. Multi-phase Flow Systems*, University of Strathclyde, Glasgow, Paper I2, Published as *Instn. Chem. Engrs. Symp. Series No.* 38.

BANERJEE, S., RHODES, E. & SCOTT, D. S. 1967 Film inversion of co-current two-phase film in helical coils. *AIChE J.* **13**, 189–191.

BUTTERWORTH, D. 1972 Air–water annular flow in a horizontal tube. *Prog. in Heat and Mass Transfer* **6**, 235–251.

BUTTERWORTH, D. & PULLING, D. J. 1973 Film flow and film thickness measurements for horizontal, annular air–water flow. AERE-R7576.

BUTTERWORTH, D. 1974 An analysis of film flow for horizontal annular flow, and condensation in a horizontal tube. *Int. J. Multiphase Flow* **1**, 671–682.

BUTTERWORTH, D. & PULLING, D. J. 1974 Mechanisms in horizontal annular air–water flow. *Symp. Multi-phase Flow Systems*, University of Strathclyde, , Glasgow, Paper A2, Published as *Instn. Chem. Engrs. Symp. Series No.* 38.

CARVER, J. R., KAKARALA, C. R. & SLOTNIK, J. S. 1964 Heat transfer in coiled tubes with two phase flow. Babcock and Wilcox Rep. 4438.

COUSINS, L. B., DENTON, W. H. & HEWITT, G. F. 1965 Liquid mass transfer in annular two phase flow. Proceeding of Two-phase Flow Symp. Exeter, U.K., Paper C4.

CRAIN, B. & BELL, K. J. 1973 Forced convection heat transfer to a two phase mixture of water and steam in a helical coil. *AIChE Symp. Series* **69**, 30–36.

FISHER, S. A. & PEARCE, D. A. 1979 A theoretical model for describing horizontal annular flows. International Seminar on Momentum, Heat and Mass Transfer in Two-phase Energy and Chemical Systems, Dubrovnik, Yugoslavia.

HEWITT, G. F., KING, R. D. & LOVEGROVE, P. C. 1962 Techniques for liquid film and pressure drop studies in annular two-phase flow. AERE-R3921.

HEWITT, G. F. & HALL TAYLOR, N. S. 1970 *Annular Two-phase Flow.* Pergamon Press, Oxford.

HUTCHINSON, P., BUTTERWORTH, D. & OWEN, R. G. 1974 Development of a model for horizontal annular flow. AERE-R7789.

KOZEKI, M. 1973 Film thickness and flow boiling for two-phase annular in a helically coiled tube. *Proc. Int. Meeting on Reactor Heat Transfer*, Karlsruhe, W. Germany, pp. 351–372.

MADDOCK, C., LACEY, P. M. C. & PATRICK, M. A. 1974 The structure of two-phase flow in a curved pipe. *Symp. Multi-phase Flow Systems*, University of Strathclyde, Glasgow, Paper J2, Published as *Instn. Chem. Engrs. Symp. Series No.* 38.

OWHADI, A., BELL, K. J. & CRAIN, B. 1968 Forced convection boiling inside helically coiled tubes. *Int. J. Heat Mass Transfer* **11**, 1779–1793.

PULLING, D. J. 1975 Private communication.

WHALLEY, P. B. & WILLIAMS, N. M. 1977 Air–water two-phase flow in a helically boiled tube. AERE-R8845.